Published in final edited form as:
Anal Chem. 2011 September 1; 83(17): 6810–6817. doi:10.1021/ac2015855.

Metabolic Differentiation of Neuronal Phenotypes by Single Cell CE-ESI-MS

Peter Nemes, **Ann M. Knolhoff**, **Stanislav S. Rubakhin**, and **Jonathan V. Sweedler***
Department of Chemistry, University of Illinois at Urbana-Champaign, 600 South Mathews Avenue, Urbana, IL 61801

Abstract

Single cell mass spectrometry (MS) is a rapidly emerging field in metabolic investigations. The inherent chemical complexity of most biological samples poses analytical challenges when using MS platforms to measure sample content without prior chemical separation. Here, a single-cell capillary electrophoresis (CE) system was coupled with electrospray ionization (ESI) MS to enable the simultaneous measurement of a vast array of endogenous compounds in over 50 identified and isolated large neurons from the *Aplysia californica* central nervous system. More than 300 distinct ion signals (*m/z* values) were detected from a single neuron in positive ion mode, 140 of which were selected for chemometric data analysis. Metabolic features were evaluated among six different neuron types (B1, B2, left pleural 1 (LPl1), metacerebral cell (MCC), R2, and R15), chosen for their various physiological functions. The results indicated chemical similarities among some neuron types (B1 to B2 and LPl1 to R2) and distinctive features for others (MCC and R15 cells). The quantitative nature of the MS platform allowed the comparison of metabolite levels for specific neurons. The CE-ESI-MS approach for examination of individual nanoliter-volume cells as described herein is readily adaptable to other volume-limited samples.

INTRODUCTION

In the field of biomarker research and discovery, methods to investigate metabolic heterogeneity among selected cells within a larger group of cells can provide unique information on cell function and fate. Although single-cell metabolomics applications are expanding,[1-4] the majority of metabolomics assays provide information about average metabolite levels in a cell population rather than levels in individual cells.[5] Of course, if the cell population is heterogeneous, the chemical complexity increases when distinct cells are pooled before measurement. These factors often hinder the study of cell-to-cell heterogeneity, which can be surprisingly broad, even for cells having similar phenotypes.[6,7] Consequently, there is a great, unmet demand for methodologies capable of investigating and quantifying the single-cell metabolome.

There are a number of analytical techniques that deliver impressive capabilities for probing the chemistry of single cells in exquisite spatial and temporal resolution. With the commercial introduction of highly specific chemical labels, optical microscopic techniques (e.g., Raman spectroscopy, far-field super-resolution fluorescence microscopy, stochastic optical reconstruction microscopy) have evolved to offer imaging resolutions below 100 nm

*To whom correspondence should be addressed. Jonathan V. Sweedler, jsweedle@illinois.edu. Phone: (217) 244-4759 Fax: (217) 265-6290 .

ASSOCIATED CONTENT Supporting Information. The Supporting Information includes detailed discussions of the experimental setup, sample analysis protocol, procedure of mathematical alignment on electropherogram data, statistical and PCA evaluation, and metabolite identification for tyrosine. This material is available free of charge via the Internet at http://pubs.acs.org.

and can routinely investigate the cellular molecular machinery in two and three dimensions in a non-destructive manner.[3,4,8] These and similar optical analytical approaches enable the direct study of chemical processes in functioning cells under native-like environments, but are only applicable to a selected array of compounds.

Mass spectrometry (MS) has proven to be an indispensible tool for metabolomic investigations, due in part to its high sensitivity and selectivity and ability to perform label-free detection. The number of MS-based approaches capable of single-cell and subcellular investigations has steadily increased,[2,9-11] and include secondary ion mass spectrometry (SIMS),[12-14] matrix-assisted laser desorption/ionization (MALDI),[1,15] scanning microprobe MALDI (SMALDI),[16] and nanostructure initiator mass spectrometry (NIMS)[17] in vacuum, as well as laser ablation electrospray ionization (LAESI)[18-20] and live video MS[21] in the ambient environment.[22] The chemical complexity observed in most living systems poses challenges for broad-range molecular identification when applying MS alone, prompting the addition of orthogonal approaches for molecular characterization.

One such integrated methodology incorporates chemical separation prior to MS detection which provides several analytical benefits. Hyphenated approaches not only simplify chemical complexity in the sample but can isolate molecular interferences from signals of interest. In turn, the analytical figures of merit are improved for qualitative and quantitative experiments. For example, data dimensionality is expanded by gaining a compound-dependent piece of information on the amount of time the analyte spends in separation. Gas chromatography, liquid chromatography, and capillary electrophoresis (CE) MS have demonstrated encouraging results in plant, animal, and human metabolomic and peptidomic applications.[10,23-26] Owing to its compatibility with small sample volumes and tolerance for high salt concentration, CE has been particularly effective for single-cell MS.[27-29]

Here we report a bioanalytical approach for the metabolic analysis and chemical classification of individual cells in the central nervous system (CNS) of *Aplysia californica* (sea hare), a widely studied model in neurobiology. Over 50 single neurons with diameters ranging from 80 to 300 μm were identified and isolated from eight animals in order to assess biological variability. A number of technical and methodological improvements were made to our previously described single-cell CE- electrospray ionization (ESI)-MS system[28] to combine label-free separation via CE with ESI-MS for the detection and quantitation of metabolites in these neurons. Metabolite concentrations were measured in single cells to probe the chemistry of neuronal diversity. Furthermore, multivariate data analysis was integrated to identify unique chemical components and patterns that correlated with cellular type and/or heterogeneity. We demonstrate that this combined analytical approach facilitates investigations of small-volume samples, including the differentiation of neuron phenotypes based on cellular chemistry.

EXPERIMENTAL SECTION

Animals and single neuron isolation

Adult *A. californica* (175–250 g in weight), purchased from the National Resource for *Aplysia* (Rosenstiel School of Marine & Atmospheric Science, University of Miami, FL, USA), were maintained in continuously circulated, aerated artificial seawater cooled to 14 °C. Eight animals were anesthetized by injecting 390 mM of aqueous magnesium chloride into the vascular cavity, equal by mass to approximately one-third of each animal's body weight. As shown in Figure 1A, ganglia and adjacent nerves were surgically dissected, enzymatically treated to remove connective tissues, and identified neurons manually isolated with a sharp tungsten needle (World Precision Instruments, Inc., Sarasota, FL) in artificial seawater that consisted of 460 mM NaCl, 10 mM KCl, 10 mM $CaCl_2$, 22 mM $MgCl_2$, 26

mM $MgSO_4$, and 10 mM 4-(2-hydroxyethyl)-1-piperazineethanesulfonic acid (HEPES), pH 7.8, mixed with glycerol (v/v, 66.7%/33.3%) to stabilize the cell membrane. For the quantitation validation, we isolated a cluster of 11 neurons, the R3-13 cluster, and treated the cell cluster as described below.

Isolated single cells were quickly rinsed with deionized water to minimize inorganic salts and extracellular metabolites on their surfaces. Neurons were placed into 5 μL of 50% (v/v) methanol solution prepared with 0.5% (v/v) acetic acid to facilitate analyte extraction and quench enzymatic processes *ex vivo*; samples were stored in the solution at −20 °C until analysis. Control experiments confirmed that this environment minimized metabolite decomposition for a period as long as two weeks and also facilitated analyte extraction into the solution (data not shown). The resulting extract solutions were centrifuged for 1 min at 2000 × g, and the aliquots directly analyzed by a CE-ESI-MS system. Further details are discussed in the Supporting Information.

Chemicals

Methanol was purchased from Fisher Scientific (Fair Lawn, NJ) and formic acid was from Thermo Scientific (Rockford, IL). All other chemicals were obtained at gradient grade or higher from Sigma-Aldrich Co. (St. Louis, MO) and were used as received unless otherwise specified. Sample extracts were kept in polymerase chain reaction vials that were purchased from MidSci (St. Louis, MO).

CE-ESI-MS platform and single-neuron analysis

Samples were analyzed by a custom-built CE-ESI-MS platform that was partially based on an earlier system.[28] Schematics of the experimental setup are shown in Figure 1B and a detailed protocol of operation is provided in the Supporting Information. A multi-channel data acquisition and control card (model USB-6008, National Instruments, Austin, TX) was operated by a personal computer (PC in Figure 1B) that executed a custom-written program (LabVIEW 8.2 interface, National Instruments); the card was programmed to output a time-dependent voltage function. This signal was converted to 20 kV by a high voltage power supply (Bertan model 30R, Spellman High Voltage Electronics Corp., Hauppauge, NY) and was directly applied across a 90-cm-long fused silica capillary (40 μm inner diameter (ID), 110 μm outer diameter (OD), Polymicro Technologies, Phoenix, AZ) for electrophoretic separations.

This separation capillary was connected to a custom-built co-axial sheath-flow ESI source that eliminated nebulizer gas. A microtee assembly (part P-875, IDEX Health & Science, Oak Harbor, WA) housed a stainless steel metal emitter (130 μm ID, 260 μm OD, part 21031A, Hamilton Company, Reno, NV) (see CE-ESI in Figure 1B). The sheath liquid (50% methanol with 0.1% formic acid) was supplied through the emitter at a 750 nL/min flow rate using a syringe pump (model 70-2000 or 55-2222, Harvard Apparatus, Holliston, MA) and a fused silica delivery capillary for the sheath flow (S in Figure 1B) (75 μm ID, 363 μm OD, Polymicro Technologies). The emitter was grounded and positioned ~2 mm in front of the skimmer plate of the mass spectrometer. The potential on this plate was adjusted to −1700 V to establish the conejet spraying mode.[30,31] The separation capillary was coaxially fed through the emitter and protruded ~50−80 μm into the Taylor cone for stable and efficient ion generation by the microelectrospray source.[32,33]

A 10 kΩ resistor was connected in series into the electrophoretic circuit to monitor the current exhibited through the CE-ESI interface. At 20 kV separation voltage, the separation capillary initially exhibited a typical current of 8.0 ± 0.2 μA for ~10–15 min and reached a plateau at 8.8 ± 0.1 μA for the remainder of the experiment. These experimental conditions

provided optimal chemical separation while minimizing solvent heating and/or electrolysis during the CE experiments for up to an hour.

For analysis, a volume of 6 nL from each neuron extract was hydrostatically introduced into the separation capillary using a custom-designed injection platform (see Figure 1B) and analyzed in at least duplicate (analytical replicates). Compounds were converted to gas-phase ions by the CE-ESI interface. The generated ions were analyzed by a micrOTOF ESI-time-of-flight (TOF) mass spectrometer or a maXis ESI-Qq-TOF tandem MS (MS/MS) mass spectrometer (Bruker Daltonics, Billerica, MA) with ~5 ppm mass accuracy and ~8000 FWHM (full width at half maximum) resolution. Mass spectra were internally calibrated with sodium formate clusters that formed in the ESI source as sodium salts eluted during CE separation. Calibrations were carried out by applying an enhanced quadratic equation with DataAnalysis (version 4.0, Bruker Daltonics). MS/MS experiments with 20–35 eV collision energies facilitated the molecular identifications.

Chemometric data analysis

Chemometric data interpretation and quantitation were performed on signal areas and intensities in selected-ion electropherograms, the former employing unsupervised principal component analysis (PCA) (Markerview 1.1; Applied Biosystems, Carlsbad, CA). Data preprocessing weighting and scaling was logarithmic and mean center, respectively. All data were plotted by a scientific visualization software package (Origin 8.0; OriginLab Corp., Northampton, MA).

Safety considerations

All high voltage connections were carefully shielded and electrically conductive parts were grounded to protect from exposure. Standard safety protocols were practiced when handling solvents and samples.

RESULTS AND DISCUSSION

The present study investigated the chemistry of a number of different neuronal networks (and corresponding neurons) in the *A. californica* CNS. With relatively large cell sizes (~50 μm to 1 mm) and small number of neurons, this mollusk is a remarkable model for investigations of memory and learning, as well as developmental biology. The functional roles of its individual neurons have been extensively studied, including their ability to modify feeding (metacerebral cell (MCC) and left pleural 1 neuron, (LPl1)), regulate mucus release (LPl1 and R2 neuron) and gut motility (B1 and/or B2 neuron), and affect egg laying (R15 neuron).[34-38] Although great progress has been made in understanding *A. californica* on the genomic, transcriptomic, proteomic, and peptidomic scales, relatively little is known concerning the cell to cell differences in its metabolome. Here, the metabolite content of individual neurons (100–300 μm in diameter) was assessed for these six genotypes, and their chemical differences surveyed.

Sample preparation involved a number of steps and is depicted in Figure 1A. Adult animals were anesthetized, sacrificed, and their CNS ganglia dissected in artificial seawater (see left image in Figure 1A). Individual neurons were identified based on size, color, and relative location in the CNS in accordance with earlier work[28] and surgically isolated (see middle image in Figure 1A). To extract endogenous compounds from these cells, the isolated neurons were placed in 50% methanol solution prepared with 0.5% acetic acid (see right image of Figure 1A). Aliquots of the extracts were directly analyzed by a custom-designed CE-ESI-MS system that was built upon an MS-based platform recently described for volume-limited samples.[28]

The CE separation step reduced the chemical complexity of the neuron samples prior to MS detection, enabling the simultaneous measurement of a vast number of compounds, both intracellular and exogenous in origin. The acquired electropherograms were initially surveyed by generating ion chromatograms in the 50–500 *m/z*-range with bins of 500 mDa. This evaluation revealed molecular features for over ~450 different accurate *m/z*-values, each corresponding to a different ionic species separated in time. Careful control experiments were conducted to analytically evaluate the cellular and analytical environments. A number of interfering chemical species were found and ascribed to polymer and plasticizer molecules, likely originating from solvent bottles, impurities present in the solutions used (methanol, water, formic acid, and acetic acid), as well as noncovalent adducts that formed *in situ* during ESI. These ions were manually excluded, and the remaining ~300 ions (*m/z* signals) were high-pass filtered at 5×10^5 counts/s.

Following this criterion, a total of 144 ionic species were then *m/z*-selected from the remaining ion list for further analysis (tabulated in Table S2). It is worth noting that this signal filtering criterion did not bias among chemical classes (e.g., osmolyte versus neurotransmitter molecules) but exhibited preference for signal intensity. Prospective developments in automation and computer processing are aimed at simultaneously monitoring the hundreds of ion signals detected. Nevertheless, the results obtained here demonstrate the broad applicability of our single-cell analytical platform and methodology. Selected ion-electropherograms were generated for each of these ions with a ± 50 mDa mass window and the corresponding electrophoretic peak maxima and area were determined for subsequent analysis.

Metabolites in single neurons

Several of the at least 300 different metabolites detected from a single neuron were identified in a multifaceted protocol. Accurate mass measurements were combined with online metabolite database searches (Metlin[39]), and positive *m/z*-matches were further confirmed in collision-induced dissociation MS/MS and migration-time comparisons against related chemical standards. A representative example is given for the identification of tyrosine in Figure S1. Using this multiplexed approach, 36 ions were ascribed with high analytical confidence (below 5 ppm absolute mass accuracy) to small metabolites, osmolytes, and classic neurotransmitters, and are detailed in Table S1.

The injection of high salts and cellular debris often affected CE migration rates, at times up to 10% relative error; these effects were reduced using the following procedure. The registered *m/z*-selected electropherograms were temporally aligned for the HEPES buffering agent (protonated $C_8H_{18}N_2O_4S$ ion measures *m/z* 239.1060 theoretical) and endogenous lysine, tryptophan, and glutathione, which provided time markers for nonlinear multi-parameter regression. An example is presented for selected MCC, LPl1, R15, and R2 neurons in Figure S3. As a result, the ~10% relative error in migration time reproducibility was reduced to <1% relative error; a 0.1% relative error is shown in Figure S1. While this data treatment significantly improves the confidence of analyte identification, it also can alter peak areas; thus, this protocol was not followed in the quantitative data analyses, including PCA. Instead, electrophoretic peak intensities and areas were obtained directly from the raw acquired data for PCA and quantitation, respectively.

Analysis of the selected-ion electropherograms revealed the neuron-specific presence of a number of ions. Representative examples are shown for the MCC, LPl1, R2, and R15 neuron extracts in Figure 2. Acetylcholine (compound **9**, see also Table S2) registered high ion counts in both the R2 and LPl1 neurons. These findings are supported by earlier results on the cholinergic and functional homolog of these neurons.[34,40] In contrast, serotonin (**13**)

was only measured in the MCC cells, an observation confirmed by independent studies reporting that MCC neurons use serotonin as a neurotransmitter.[41,42] Interestingly, the ion *m/z* 267.1333 (unknown identity) was exclusively found in the R15 neurons. This unknown mass matches the formula $C_{13}H_{18}N_2O_4$ within 1 ppm accuracy, and may correspond to the dipeptide ThrPhe (or PheThr); future work will validate the assignment of this cell-specific metabolite.

Other compounds populated the cell extracts in fairly uniform ion counts. Glycine betaine (**32**) and proline betaine were generally detected in high abundance in most of the interrogated cells (see Figure 2). In agreement with our observations, the former compound is a known intracellular osmolyte and is present at 100-300 mM in the intracellular space.[43] These results impart confidence that our CE-ESI-MS platform not only measured endogenous metabolites from neuron extracts, but also yielded data that represents the biological composition of the neurons.

Metabolic heterogeneity among neurons and neuron types

Our results provided an opportunity to investigate the cellular heterogeneity and classify individual neurons at a chemical level. PCA was employed to further distinguish the cell types. Seven to nine individual neurons were isolated from different *A. californica* (biological replicates) and were analyzed in duplicate (analytical replicate) for each of the following neuron types: B1, B2, MCC, LPl1, R2, and R15. Using PCA on 144 different selected ions (see Table S2), the vast dataset from these experiments (over ~14,000 ion intensity values) was mathematically transformed into orthogonal components to reduce data dimensionality, helping to reveal underlying chemical correlations among the studied neuron phenotypes.

PCA of the CE-ESI-MS data demonstrated that the neurons exhibited individual as well as phenotypic differences in their chemistry. The PCA outcomes are shown in Figure 3. The first two principal components explained ~70% of the total variance among the measured ion intensities. The biological variability (~25–50% S.E.M. for most cell types, see Figure S4) exceeded the analytical reproducibility (below 20%, see Supporting Information); thus, only single measurements are included in Figure 3 to aid visual data interpretation. Notably, data points from the LPl1 and R2 neuron extracts form overlapping clusters in the first two orthogonal dimensions. Likewise, most B1 and B2 single cells are virtually indistinguishable in Figure 3. These PCA results demonstrate that these neuron pairs possess similar chemical compositions. In contrast, the MCC and R15 data clusters populated in distant quadrants of the scores plot, indicating significantly different metabolic profiles for these neurons as compared to the other four cell types.

Our chemical observations add an important piece of evidence to the existing knowledge about the physiological differences in neuron phenotypes. The PCA results confirmed that, even though located in nonsymmetrical ganglia, the LPl1 and R2 neurons were biochemically homologous. Previously, the evidence that these cells were homologous included morphological observations on the almost symmetrical axonal trees over the body walls of the animal, and their shared cholinergicity.[34]

Chemical heterogeneity was observed for single neurons within the same neuronal type. As shown in Figure 3, the R2 and LPl1 neurons arranged into tight data clusters (small cluster radius) whereas the variance appeared to increase in the following order: R15, LPl1 < MCC < B2 << B1. Moreover, PCA revealed that three of the B1 and one of the B2 neurons were chemically different to a noticeable degree from the others (Figure 3). Because cell isolations and chemical analyses were performed with sufficient confidence, the observed

cellular heterogeneity may be explained by biological variation among animals and their specific behavioral and physiological state.

Metabolites correlating with the observed chemical relations among cells and cell phenotypes were screened during PCA. Referring to the loading plot in Figure 3, we can distinguish the ions that made the highest contribution in differentiating the studied neurons. For example, the histamine (**1**) and serotonin (**13**) ions occupy the left lower quadrant of the plot. These ions are specific to MCC neurons. In contrast, acetylcholine (**9**), in the top right region, has the highest PC2 value. This piece of information allows for the screening of cholinergic cells. Notably, the glycine betaine (**32**) and proline betaine (**33**) are in close vicinity to the origin, which indicates low specificity for any of the studied neurons. This observation is in accordance with both compounds being intracellular osmolytes and present in high abundance in marine animals, including sea slugs.[43,44]

Metabolite quantitation in individual cells

This bioanalytical platform also enabled the quantitation of endogenous metabolites in the neuron extracts. The average CE-ESI-MS analysis time was ~50 min for each sample, amounting to more than 100 h of continuous data collection for all neuron extracts. Obviously, this low sample throughput required robust instrument performance for an extended period of time, and manual system operation imposed stringent operation protocols on users. To gauge the cumulative error associated with manual sample analysis, the instrument signal response was rigorously tested for day-to-day variations. As detailed in the Supporting Information, the analytical uncertainly was <15% for a chemical standard solution. These cautious steps in combination with randomized sample analysis ensured data collection in a chemically representative and quantitative manner and eliminated systematic bias.

The CE-ESI-MS platform was also characterized for analytical figures of merit. The limit of detection was below 50 nM (300 amol analyzed) and the linear range for quantitation spanned over three orders of magnitude for acetylcholine, histamine, and dopamine (data not shown). These performance features were in good agreement with results obtained previously on a similar system,[28] and also presented an opportunity to quantify endogenous compounds present in biologically relevant concentrations in the single neurons.

External concentration-calibration allowed the measurement of any detected compound that was also available as a chemical standard. Linear calibration curves are shown for serine and glutamic acid on a log-log scale in Figure 4. The linear regression coefficients were above 0.99 for a three-orders-of-magnitude concentration range (see solid lines). Using this information, the metabolite levels were calculated in six different neurons from each of the B1, LPl1, R2, and R15 phenotypes. In addition, this experiment was extended for the nonglutamergic R3–13 ganglion as well for comparison with literature data. Metabolite levels are depicted for the individual cells in Figure 4 and tabulated in Table 1 for the extract solutions as well as calculated for the specific cells types; the latter was calculated using three assumptions: spherical cell shape (see neuron diameters in Table 1), homogeneous intracellular metabolite distribution *in vivo*, and homogeneous analyte distribution between the cell and the extract after extraction. This data indicated that on average, the intracellular glutamic acid concentration was ~11.4 mM in the R2 and 4.4 mM (± 20%) in the R3-13 neurons. These findings are in agreement with several independent investigations,[45-47] corroborating our single-cell metabolomic quantitation results.

On an individual neuron level, metabolite concentrations exhibited variance not only among neuron types but also among neurons of the same type. For example, the glutamic acid levels were found to be the lowest in the B1 and highest in the LPl1 cell extracts (see Figure

4), with the intracellular concentration difference reaching one order of magnitude between the two genotypes (see Table 1). In contrast, the serine levels did not appear to significantly change with cell type but rather, with neuron individuality. For example, the concentration difference was almost a magnitude greater between the B1 neurons **a** and **c** (see Table 1). Optical investigations during the isolation work did not indicate a noticeable difference in the size of these neurons that would account for the observed divergence in metabolite levels. Furthermore, the glutamic acid/serine concentration ratio (see Table 1) was exceptionally high in the B1 neuron **b** in comparison to other cells of the same type. This piece of information may reveal an unusual metabolism for this cell and/or its host, but can also indicate a natural response to a change in environmental factors.

These results further stress the importance of quantitatively assessing cell chemistry at a single-cell resolution. The cellular heterogeneity that the present measurements indicate also underlines the significance of single-cell measures in statistically significant numbers in order to adequately represent the biochemical state of a given cell population.

CONCLUSIONS

The interrogation of cell individuality and phenotype by the herein described approach adds chemical insight to cellular bioanalyses. We have demonstrated label-free selective analysis, metabolite quantitation and identification with high analytical confidence, and chemical screening of over 50 isolated and identified single cells (80–300 μm in diameter) from the CNS of one of the most investigated neurobiological models, *A. californica*. Unsupervised chemometric analysis of the obtained data revealed differences in metabolite content not only among cell types but individual neurons of the same type. We expect that single-cell studies on the mammalian CNS will show similar and striking cell-to-cell heterogeneity in chemistry; for example, the larger neurons in the human CNS are on a similar scale (between 50–150 μm), the approach should work directly with such neurons.

Although single cell isolation presents a bottleneck in the current experimental workflow, enhancements in single cell isolation and manipulation technologies have the potential to increase analytical throughput and broaden biological applicability. The combination of continuous cell delivery and lysis with microfluidic devices poses an elegant solution, and this approach has recently demonstrated the feasibility of protein analysis with sampling rates as high as 12 cells per minute.[29] Microfabrication and micropatterning open opportunities to mimic the *in vivo* extracellular environment, allow the separation of spatial and temporal factors in cell regulation, and apply rapid chemical nutrient gradients. Furthermore, the physical dimensions of microchannels compare with many mammalian neurons (~10–20 μm in diameter), and so their combination with the CE-ESI-MS platform should allow automated neuronal sampling with less dilution and perhaps greater automation. The resulting small-molecule analysis technique is expected to complement peptidomic and proteomic efforts in model organisms of higher CNS complexity, including *Caenorhabditis elegans* and *Drosophila melanogaster*.

Advances in software frameworks for mass spectral data exploration are expected to greatly complement research efforts in metabolomics, including the present single-cell analysis approach. CE-ESI-MS of the neurons studied in this work generated ~200 GB of electropherogram data in the single-stage MS mode. Interpreting this large amount of data demands significant physical computing power as well as the availability of sophisticated software platforms. In addition, manual data analysis revealed that our CE-ESI-MS platform registered molecular features over a broad range of peak widths (ranging from 5 to ~60 s); this, in combination with occasional low migration time reproducibility among analyses, challenged molecular feature detection using currently available software packages.

Sophisticated mathematical algorithms such as open-source XCMS,[48] MZmine,[49] MathDAMP,[50] and most recently, metaXCMS[51] data-analysis tool boxes are promising means to aid the analytical workflow. Reduction in the dataset size, exploration of spectral features with high temporal resolution, and the feasibility of direct statistical analysis on non-targeted datasets are apparent advantages of similar software venues for metabolomics. Once spectral features are identified, ideally these software platforms would allow the direct screening of on-line high mass-resolution MS and tandem MS metabolite depositories such as the Metlin[39] database used in this study for automated metabolite identification.

Supplementary Material

Refer to Web version on PubMed Central for supplementary material.

Acknowledgments

The project described was supported by the National Science Foundation (NSF) under award number CHE-0400768, the National Institute of Neurological Disorders and Stroke (NINDS), Award No. NS031609, and the National Institute of Dental and Craniofacial Research (NIDCR) and the Office of Director (OD), National Institutes of Health (NIH), Award No. DE018866. The content is solely the responsibility of the authors and does not necessarily represent the official views the NSF, NINDS, NIDCR or the National Institutes of Health. The authors thank Xiying Wang for the single neuron preparation work, Stephanie Baker for assistance in the preparation of this publication, and the UIUC School of Chemical Sciences machine shop for providing various components for the construction of the CE-ESI system.

REFERENCES

(1). Rubakhin SS, Garden RW, Fuller RR, Sweedler JV. Nat. Biotechnol. 2000; 18:172–175. [PubMed: 10657123]

(2). Rubakhin SS, Romanova E, Nemes P, Sweedler JV. Nat. Methods. 2011; 8:S20–S29. [PubMed: 21451513]

(3). Brehm-Stecher BF, Johnson EA. Microbiol. Mol. Biol. Rev. 2004; 68:538–559. [PubMed: 15353569]

(4). Huang B, Wang WQ, Bates M, Zhuang XW. Science. 2008; 319:810–813. [PubMed: 18174397]

(5). Griffiths WJ, Koal T, Wang YQ, Kohl M, Enot DP, Deigner HP. Angew. Chem.-Int. Edit. 2010; 49:5426–5445.

(6). Newman JRS, Ghaemmaghami S, Ihmels J, Breslow DK, Noble M, DeRisi JL, Weissman JS. Nature. 2006; 441:840–846. [PubMed: 16699522]

(7). Stahlberg A, Bengtsson M. Methods. 2010; 50:282–288. [PubMed: 20064613]

(8). Engler AJ, Sen S, Sweeney HL, Discher DE. Cell. 2006; 126:677–689. [PubMed: 16923388]

(9). Rubakhin SS, Sweedler JV. Nat. Protoc. 2007; 2:1987–1997. [PubMed: 17703210]

(10). Amantonico A, Urban PL, Zenobi R. Anal. Bioanal. Chem. 2010; 398:2493–2504. [PubMed: 20544183]

(11). Tsuyama N, Mizuno H, Masujima T. Anal. Sci. 2011; 27:163–170. [PubMed: 21321439]

(12). Monroe EB, Jurchen JC, Lee J, Rubakhin SS, Sweedler JV. J. Am. Chem. Soc. 2005; 127:12152–12153. [PubMed: 16131155]

(13). Fletcher JS, Lockyer NP, Vaidyanathan S, Vickerman JC. Anal. Chem. 2007; 79:2199–2206. [PubMed: 17302385]

(14). Kurczy ME, Piehowski PD, Van Bell CT, Heien ML, Winograd N, Ewing AG. Proc. Natl. Acad. Sci. U. S. A. 2010; 107:2751–2756. [PubMed: 20133641]

(15). Amantonico A, Urban PL, Fagerer SR, Balabin RM, Zenobi R. Anal. Chem. 2010; 82:7394–7400. [PubMed: 20707357]

(16). Bouschen W, Schulz O, Eikel D, Spengler B. Rapid Commun. Mass Spectrom. 2010; 24:355–364. [PubMed: 20049881]

(17). Northen TR, Yanes O, Northen MT, Marrinucci D, Uritboonthai W, Apon J, Golledge SL, Nordstrom A, Siuzdak G. Nature. 2007; 449:1033–U1033. [PubMed: 17960240]
(18). Nemes P, Vertes A. Anal. Chem. 2007; 79:8098–8106. [PubMed: 17900146]
(19). Shrestha B, Vertes A. Anal. Chem. 2009; 81:8265–8271. [PubMed: 19824712]
(20). Shrestha B, Nemes P, Vertes A. Appl. Phys. A Mater. Sci. Process. 2010; 101:121–126.
(21). Mizuno H, Tsuyama N, Harada T, Masujima T. J. Mass Spectrom. 2008; 43:1692–1700. [PubMed: 18615771]
(22). Cooks RG, Ouyang Z, Takats Z, Wiseman JM. Science. 2006; 311:1566–1570. [PubMed: 16543450]
(23). Dunn WB, Ellis DI. Trends Analyt. Chem. 2005; 24:285–294.
(24). Ramautar R, Mayboroda OA, Somsen GW, de Jong GJ. Electrophoresis. 2011; 32:52–65. [PubMed: 21171113]
(25). Fiehn O. Plant Mol. Biol. 2002; 48:155–171. [PubMed: 11860207]
(26). Kell DB. Drug Discov. Today. 2006; 11:1085–1092. [PubMed: 17129827]
(27). Hofstadler SA, Severs JC, Smith RD, Swanek FD, Ewing AG. Rapid Commun. Mass Spectrom. 1996; 10:919–922. [PubMed: 8777325]
(28). Lapainis T, Rubakhin SS, Sweedler JV. Anal. Chem. 2009; 81:5858–5864. [PubMed: 19518091]
(29). Mellors JS, Jorabchi K, Smith LM, Ramsey JM. Anal. Chem. 2010; 82:967–973. [PubMed: 20058879]
(30). Cloupeau M, Prunetfoch B. J. Electrost. 1990; 25:165–184.
(31). Juraschek R, Rollgen FW. Int. J. Mass spectrom. 1998; 177:1–15.
(32). Valaskovic GA, Murphy JP, Lee MS. J. Am. Soc. Mass. Spectrom. 2004; 15:1201–1215. [PubMed: 15276167]
(33). Nemes P, Marginean I, Vertes A. Anal. Chem. 2007; 79:3105–3116. [PubMed: 17378541]
(34). Rayport SG, Ambron RT, Babiarz J. J. Neurophysiol. 1983; 49:864–876. [PubMed: 6189980]
(35). Bablanian GM, Weiss KR, Kupfermann I. Behav. Neural Biol. 1987; 48:394–407. [PubMed: 3689286]
(36). Rosen SC, Weiss KR, Goldstein RS, Kupfermann I. J. Neurosci. 1989; 9:1562–1578. [PubMed: 2723741]
(37). Lloyd PE, Kupfermann I, Weiss KR. J. Neurophysiol. 1988; 59:1613–1626. [PubMed: 2838590]
(38). Skelton ME, Koester J. J. Comp. Physiol. A-Sens. Neural Behav. Physiol. 1992; 171:141–155.
(39). Smith CA, O'Maille G, Want EJ, Qin C, Trauger SA, Brandon TR, Custodio DE, Abagyan R, Siuzdak G. Ther. Drug Monit. 2005; 27:747–751. [PubMed: 16404815]
(40). Eisenstadt M, Goldman JE, Kandel ER, Koike H, Koester J, Schwartz JH. Proc. Natl. Acad. Sci. U. S. A. 1973; 70:3371–3375. [PubMed: 4519630]
(41). Weinreich D, McCaman MW, McCaman RE, Vaughn JE. J. Neurochem. 1973; 20:969–976. [PubMed: 4697896]
(42). Hatcher NG, Zhang X, Stuart JN, Moroz LL, Sweedler JV, Gillette R. J. Neurochem. 2008; 104:1358–1363. [PubMed: 18036151]
(43). Grant SC, Aiken NR, Plant HD, Gibbs S, Mareci TH, Webb AG, Blackband SJ. Magn. Reson. Med. 2000; 44:19–22. [PubMed: 10893516]
(44). Pierce SK, Rowland LM. Physiol. Zool. 1988; 61:205–212.
(45). Iliffe TM, McAdoo DJ, Beyer CB, Haber B. J. Neurochem. 1977; 28:1037–1042. [PubMed: 16987]
(46). Brownstein MJ, Saavedra JM, Axelrod J, Zeman GH, Carpenter DO. Proc. Natl. Acad. Sci. U. S. A. 1974; 71:4662–4665. [PubMed: 4373726]
(47). Drake TJ, Jezzini S, Lovell P, Moroz LL, Tan WH. J. Neurosci. Methods. 2005; 144:73–77. [PubMed: 15848241]
(48). Smith CA, Want EJ, O'Maille G, Abagyan R, Siuzdak G. Anal. Chem. 2006; 78:779–787. [PubMed: 16448051]
(49). Pluskal T, Castillo S, Villar-Briones A, Oresic M. BMC Bioinformatics. 2010; 11

(50). Baran R, Kochi H, Saito N, Suematsu M, Soga T, Nishioka T, Robert M, Tomita M. BMC Bioinformatics. 2006; 7

(51). Tautenhahn R, Patti GJ, Kalisiak E, Miyamoto T, Schmidt M, Lo FY, McBee J, Baliga NS, Siuzdak G. Anal. Chem. 2011; 83:696–700. [PubMed: 21174458]

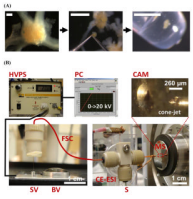

Figure 1.

Single-neuron analysis by CE-ESI-MS. (A) Optical images show (left) the abdominal ganglion removed from *A. californica*, (middle) manual isolation of an identified R2 neuron, and (right) the solution-extraction of the intracellular analytes. White scale bars = 1 mm. (B) Single-cell analysis platform included a regulated high voltage power supply (HVPS) remotely controlled by a personal computer (PC), SST sample and buffer vials (SV and BF, respectively) for sample-loading and separation in the fused silica capillary (FSC), a custom-designed coaxial sheath-flow CE-ESI interface (CE-ESI) hyphenated to a mass spectrometer (MS), and a 6.3× stereomicroscope (CAM) to observe and operate the electrospray in the cone-jet spraying mode. White bars denote the scale.

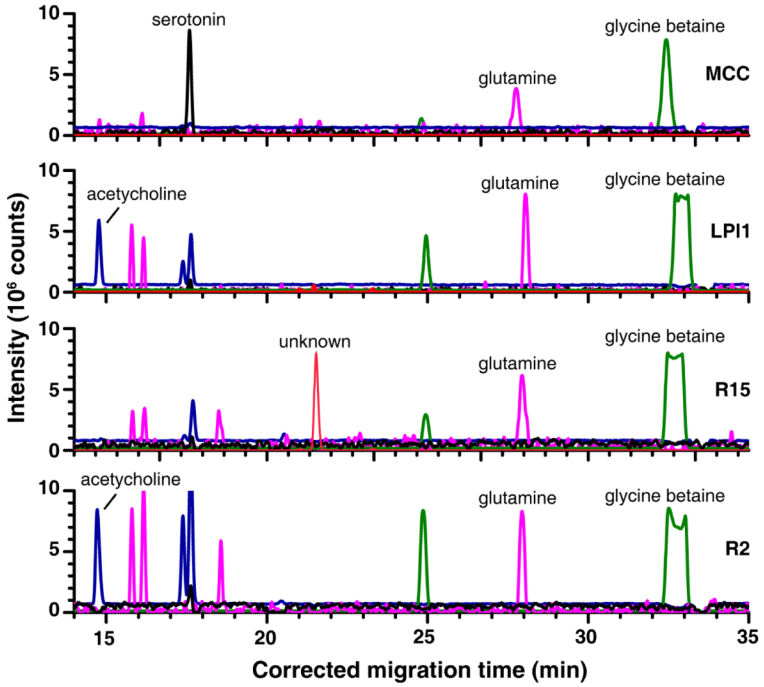

Figure 2.

Metabolic differences observed among neuronal types. Representative selected-ion electropherograms are shown for a ±5 mDa *m/z* window (signal multiplied by indicated factor): *m/z* 146.118 (1×, acetylcholine, compound **9**),); *m/z* 177.103 (2×, serotonin, **13**); *m/z* 267.133 (2×, unknown); *m/z* 147.077 (5×, glutamine, **26**)*;* and *m/z* 118.087 (0.2×, glycine betaine, **32**). Migration times were corrected as detailed in Figure S3 and the Supporting Information.

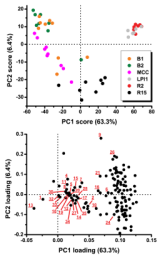

Figure 3.

Chemometric evaluation of neuronal heterogeneity and phenotype. (Top) The PCA scores plot revealed chemical differences between individual neurons and neuron types. Each data point corresponds to a different single cell. (Bottom) The loading plot helped locate characteristic metabolites among the cells. Each data point corresponds to a molecular feature identified in the *m/z*-selected electropherograms. Numbers correspond to identified metabolites, which are listed in Table S1.

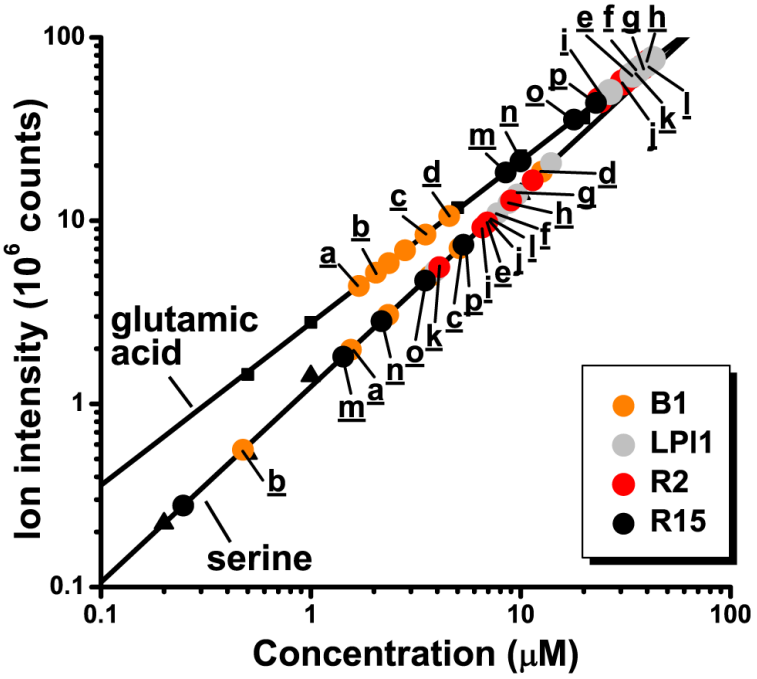

Figure 4.

Label-free quantitation of glutamic acid (■) and serine (▲) in single B1, LPl1, R2, and R15 neurons. Letters (underlined) identify single neurons and are listed in Table S3. Calibration curves for ion intensity, *I* (counts), and concentration, *c* (μM), from linear fittings were $\log(I) = 11.75 + 0.88 \log(c)$ for glutamic acid ($R^2 = 0.998$) and $\log(I) = 12.49 + 1.07 \log(c)$ for serine ($R^2 = 0.997$). The relative standard deviation was below 20% for the calibration data points.

Table 1

Representative examples for glutamic acid and serine concentrations measured in identified isolated neurons from the *A. californica* CNS.

Neuron		Glutamic acid	Serine	Concentration
Identifier	Phenotype	(μM)[a] / (mM)[b]	(μM)[a] / (mM)[b]	ratio*
a	B1	1.7 / 0.6	1.5 / 0.5	1.1
b	B1	2.0 / 0.7	0.5 / 0.2	4.0
c	B1	3.5 / 1.2	5.1 / 1.8	0.7
d	B1	4.6 / 1.6	12.6 / 4.5	0.4
e	LPl1	34.0 / 12.0	6.9 / 2.5	4.9
f	LPl1	36.1 / 12.8	7.8 / 2.7	4.6
g	LPl1	36.9 / 13.1	9.6 / 3.4	3.8
h	LPl1	39.4 / 13.9	8.7 / 3.1	4.5
i	R2	23.7 / 8.4	6.5 / 2.3	3.6
j	R2	33.5 / 11.8	6.8 / 2.4	4.9
k	R2	30.6 / 10.8	4.1 / 1.4	7.4
l	R2	40.9 / 14.5	6.9 / 2.4	5.9
m	R15	8.5 / 10.1	1.4 / 1.7	6.1
n	R15	9.9 / 11.9	2.2 / 2.6	4.5
o	R15	18.0 / 21.5	3.5 / 4.2	5.1
p	R15	22.9 / 27.3	5.3 / 6.4	4.3

Concentrations are given for [a]the extract solution and [b]cellular concentration, assuming a homogeneous distribution and a spherical average cell diameter of 100 μm for the B1 neurons, 200 μm for the R15 neurons, and 300 μm for the LPl1 and R2 neurons. External calibration curves are shown in Figure 4. The relative standard deviation for quantitation was below 15% for chemical standards.

*Metabolite ratios were calculated by dividing glutamic acid levels by serine concentrations.